Advanced Powder Technology 31 (2020) 843–847

Contents lists available at ScienceDirect

Advanced Powder Technology

journal homepage: www.elsevier.com/locate/apt

Order from Chaos: Dynamics of density segregation in continuously aerated granular systems

Jun Oshitani [a,*], Shogo Hayashi [b], Derek Y.C. Chan [c,d]

[a] Department of Applied Chemistry and Biotechnology, Okayama University of Science, 1-1 Ridai-cho, Kita-ku, Okayama 700-0005, Japan
[b] Division of Applied Chemistry, Graduate School of Natural Science and Technology, Okayama University, 3-1-1 Tsushima-naka, Kita-ku, Okayama 700-8530, Japan
[c] Department of Mathematics, Swinburne University of Technology, Hawthorn 3122, VIC, Australia
[d] School of Mathematics and Statistics, University of Melbourne, Parkville 3010, VIC, Australia

ARTICLE INFO

Article history:
Received 22 July 2019
Received in revised form 18 November 2019
Accepted 2 December 2019
Available online 20 December 2019

Keywords:
Fluidized bed
Density segregation
Granular system
Time dependence

ABSTRACT

Under continual disturbance such as vibration, tumbling, flow or aeration, granular or powder systems can display solid or fluid like behavior. Using a well-mixed system of same size (0.2 mm) non-cohesive glass beads and iron powder, we show that gentle aeration can completely segregate the components thereby reducing the entropy of mixing to create near total order from an initially chaotic mixture. We quantify the time dependence of the segregation process and identify two dynamic pathways that dominate depending on the intensity of the aeration. Such findings can facilitate the search for energy efficient methods to process granular systems in pharmaceutical, mining and waste recovery industries.

A report by the US National Research Council on Condensed Matter and Material Physics 2010, intended as "a decadal survey of opportunities and challenges", noted that "much of the richness of the world around us arises from conditions far from equilibrium" and studies in "condensed matter and materials physics is uniquely positioned to spearhead progress in the field of far-from-equilibrium behavior" [1]. Common and well-known examples of such far-from-equilibrium phenomena are the Brazil Nut Effect in which granular mixtures of different size particles segregate when shaken continually [2,3], the Christmas Tree Effect of segregation when a free-flowing particulate mixture is poured onto a heap [4], and the tumbling segregation of such a mixture when it is held in a partially filled cylindrical container that is rotated about the cylindrical axis [5,6]. The complex 3D spatial structures of these segregated states are intriguing and visually very appealing. Their formation depends on factors such as particle size and density ratio, air pressure, flow rate and frictional interactions with container walls. Being able to understand and control such behavior of granular media may provide the key to novel applications that would be relevant to pharmaceutical formulations [7], catalysis [8], mineral processing [9,10], sorting in sustainable recycling methods [11,12] and the general handling and transportation of such materials. For examples, with monodisperse non-cohesive granular systems, progress has been made in the development of constitutive equations that can predict structure of granular flow down an inclined base [13].

However, the focus on spatially complex 3D segregated states are perhaps of less relevance if the objective is to separate components of such mixtures. For mixtures with different size components, segregation by sieving is the obvious approach, but for mixtures of similar size constituents, the density difference can be exploited. Here, we investigate the dynamics and mechanisms of segregation due to relatively gentle aeration of a 50:50 mixture of non-cohesive spherical glass beads and iron powder. We determine the conditions under which the mixing of an initially random mixture can be reduced to achieve a near totally ordered state of complete segregation and investigate the time-dependent dynamics of how this is comes about.

A cylindrical container of inner diameter 100 mm was filled to a depth of 100 mm with a random mixture of glass beads (GB) and iron powder (IP) that are spherical particles of 0.18–0.21 mm diameter. A uniform air stream was injected into the bottom of the container at a controlled superficial air velocity u (= [injected air volume per unit time] / [container cross-sectional area]) corresponding to a pressure drop P across the powder bed. See Supplementary material for details about the experimental equipment and experimental protocol. In Fig. 1, we show measurements of the pressure-air velocity relationship over the complete range of glass beads volume fraction, V_{GB} or iron powder volume fraction,

* Corresponding author.
E-mail address: oshitani@dac.ous.ac.jp (J. Oshitani).

https://doi.org/10.1016/j.apt.2019.12.002

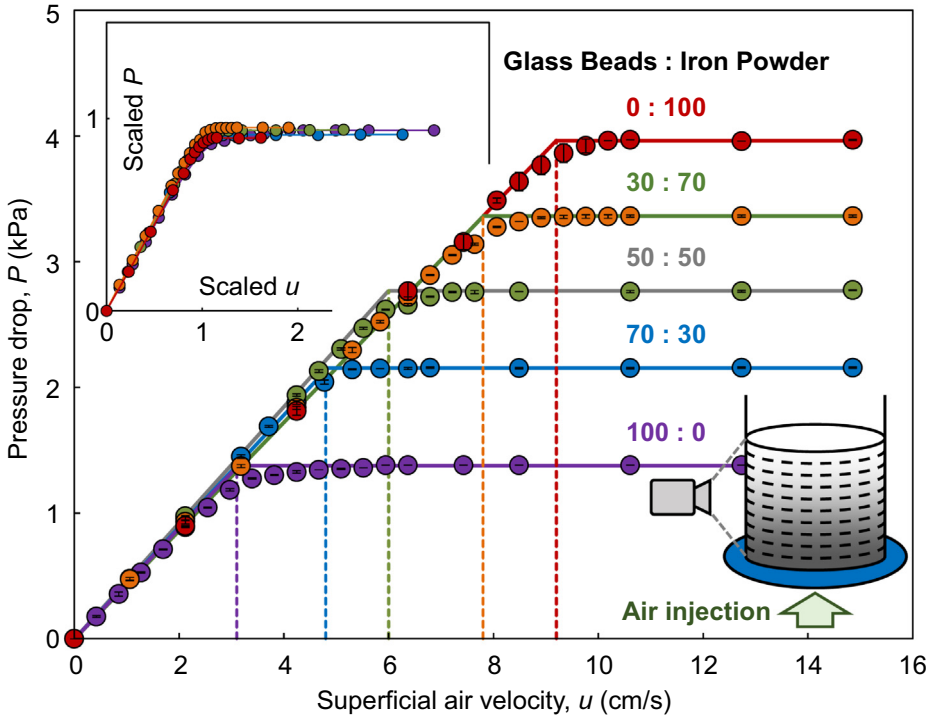

Fig. 1. Variation of the pressure drop, P across an equal size glass beads and iron powder mixture with superficial velocity, u at the indicated compositions. At small u, P increases linearly with u in the fixed bed regime and then enters the fluidized bed regime in which P is constant at large u. The transition between these 2 regimes occurs at the minimum fluidization velocity, u_{mf} that is obtained by extrapolation. See the Supplementary material for values. Inset: Data in the main figure in which u is scaled by u_{mf} and P is scaled by $P_{mf} \equiv \rho_{bed}\, gh$, the total bed mass per unit area of the container (see text for details).

$V_{IP} = 1 - V_{GB}$. At low air velocities, the linear relationship between the air velocity, u and the pressure drop, P indicated that the powder bed behaved like a solid porous material. This is confirmed by the observation that the pressure-velocity relation followed the linear Darcy Law for which the permeability is given by the Carmen-Kozeny equation [14] with a porosity, $\varepsilon = 0.4$ that is characteristic of a random medium of packed hard spheres. However, when the air velocity was increased beyond a critical value, namely, the minimum fluidization velocity, u_{mf}, the pressure then remained at a constant value, P_{mf} that is characteristic for the pressure drop of a Newtonian fluid flowing along a pipe. Thus depending on the air velocity, the GB + IP mixture could behave as a solid at low air velocities or as a liquid at high air velocities.

The observed variation of the minimum fluidization velocity, u_{mf} with composition of the mixture can be predicted from the corresponding values of the pure components, u_{mf} (GB) = 3.1 cm/s and u_{mf} (IP) = 9.2 cm/s using the effective medium formula $u_{mf}^{eff} = u_{mf}$ (IP) $V_{IP} + u_{mf}$ (GB) V_{GB} (see Supplementary material). Furthermore, the pressure–velocity results all scaled to a master curve, Fig. 1 inset, using the velocity scale, u_{mf}^{eff} and the pressure scale, $P_{mf} = (\rho_{IP}\, V_{IP} + \rho_{GB}\, V_{GB})gh \equiv \rho_{bed}\, gh$, where ρ_{GB} (1.5 gm/cm^3) and ρ_{IP} (4.5 gm/cm^3) are the bed densities of the pure glass bead and the pure iron powder, g is the gravitational acceleration and h is the bed height. These results indicate that the chosen GB + IP system could be well characterized and modelled as non-cohesive hard spheres. Since segregation occurs for $u > u_{mf}$, the results in Fig. 1 are valid only for a short period of aeration time in this regime.

For a 50:50 GB + IP mixture, the minimum fluidization velocity was 6.0 cm/s. For air velocities between this value and the minimum fluidization velocity of the pure IP of 9.2 cm/s, extended periods of aeration would result in increasing degree of segregation between the components. The most notable and potentially useful results occurred for air velocity in the range 9.2 cm/s < u < 12 cm/s. An overview of the behavior has been summarized in the sequence of snap shots in Fig. 2 that are taken from video recordings (available in the Supplementary material) at u = 9.2, 9.8, 10.4, 11.2 and 11.8 cm/s. Two distinct regimes of the time dependence of the segregation phenomenon are evident. After ~110 s of aeration at u = 9.2 and 9.8 cm/s, the initially well-mixed bed of 50:50 GB + IP segregated into an upper phase comprising almost 100% of the lighter GB and a lower phase comprising almost 100% of the heavier IP. A similar behavior was observed at u = 10.4, 11.2 and 11.8 cm/s, but the segregation process took about twice as long, ~240 s, to complete. As expected, for even higher air velocities, above 12 cm/s, the degree of segregation, if any, was small as the high airflow kept the powder bed randomized.

To obtain quantitative information about the dynamics of the segregation process and to quantify how the bed density evolved with time as the aeration proceeded, we stopped the airflow after different aeration periods and recorded the vertical variation of the composition of the powder mixture. We do so by excavating the 100 mm powder bed from the top in 10 mm layers and characterized the composition in each layer in terms of the volume fraction of iron powder, $V_{IP}(L)$ in layer L, with L = 1 being the top most layer and L = 10 the bottom layer. The corresponding volume fraction of glass beads is $V_{GB}(L) \equiv 1 - V_{IP}(L)$. Such data on the time variation of the composition distribution of the aerated bed for air velocities in the range 9.2 cm/s < u < 12 cm/s and different aeration times up to 600 s are summarized in Fig. S2 of the Supplementary material.

A succinct overview of such extensive results on the spatial-temporal evolution of an initially random 50:50 mixture can be obtained by considering the segregation efficiency, E

$$E = \frac{1}{10}\left\{\sum_{L=1}^{5}\frac{50 - V_{IP}(L)}{50} + \sum_{L=6}^{10}\frac{V_{IP}(L) - 50}{50}\right\} \times 100\% \qquad (1)$$

where $V_{IP}(L)$ is expressed as a percentage. For a well-mixed non-segregated mixture, $V_{IP}(L)$ = 50% for all layers, L and thus Eq. (1)

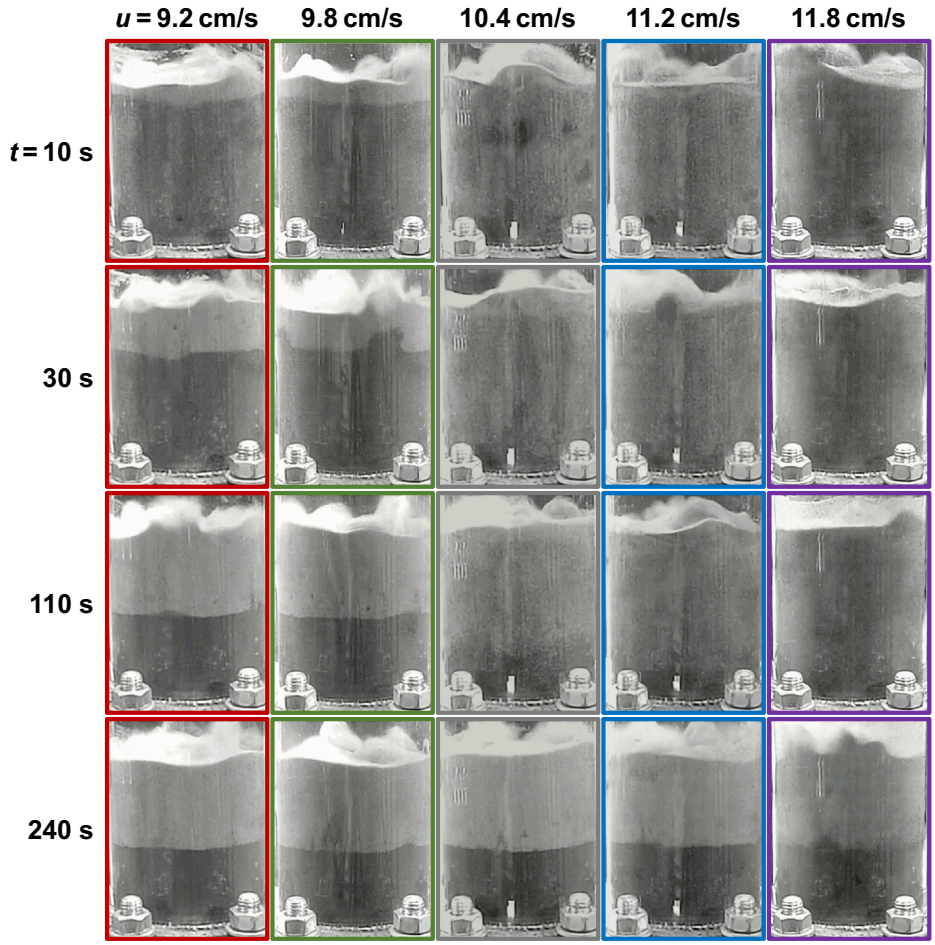

Fig. 2. Snap shots from video recordings of an initially well-mixed 50:50 glass beads (white) and iron powder (black) bed showing how the segregation develops at different superficial velocities, u. See the Supplementary material for the video.

gives E = 0%. When the GB + IP mixture segregates perfectly into an upper GB layer and a lower IP layer, V_{IP} (L) = 0% for the upper five layers, L = 1 ~ 5, and V_{IP} (L) = 100% for the lower five layers, L = 6 ~ 10 so that E = 100% denotes perfect segregation. The variation of E with air velocity, u over a total aeration time of 600 s is shown in Fig. 3. From this we see that highly efficient, ~95% segregation can be achieved with air velocities between 9.8 cm/s < u < 11.8 cm/s, whereas the segregation efficiency falls away rapidly outside this velocity range. Thus, there is a well-defined range of air velocity, u within which near total order of complete segregation can be achieved from an initially chaotic random mixture.

The results in Fig. 3 are for a total aeration time of 600 s. However, it is also important to determine the precise aeration time needed to achieve a desired level of segregation efficiency. From the extensive data on the variation of the mixture composition with bed depth after different aeration times summarized in Fig. S2 of the Supplementary material, we can construct the time dependence of the segregation efficiency, E at different aeration velocities shown in Fig. 4. From this we can see that using an air velocity at the lower range (9.2 cm/s and 9.8 cm/s) will achieve faster initial segregation whereas for aeration at higher air velocities (10.4 cm/s to 11.8 cm/s), the initial segregation process is slower, but the final segregation efficiency that can be achieved is slightly higher at ~95% compared to ~90%.

To gain insight into the reason for a faster initial segregation rate at the lower end of the velocity range 9.2 cm/s < u < 11.8 cm/s, we determine the initial flux of iron powder within the first 10 s of aeration as a function of depth in the bed. The change in the IP volume fraction, ΔV_{IP} (L) in layer L after 10 s can be expressed in terms of the flux of IP, $J(L-1, L)$ from layer $(L-1)$ into layer L and the flux of IP, J(L, L + 1) from layer L into layer $(L+1)$ by

$$\Delta V_{IP}(L) = J(L-1, L) - J(L, L+1) \quad (2)$$

Thus the initial fluxes $J(L-1, L)$, estimated as average values within the initial 10 s, can be calculated from the measured values of ΔV_{IP} (L) using the obvious boundary conditions: $J(0, 1) = 0 = J(10, 11)$. These estimates of the initial fluxes are shown in the inset of Fig. 4. The corresponding fluxes for the glass beads (GB) can be determined in a similar way since $\Delta V_{GB}(L) \equiv 1 - \Delta V_{IP}$ (L). Small discrepancies between the fluxes reflect slight deviations of the initial local volume fraction from the bulk average of 50:50.

Now it is evident that at air velocities u = 10.4, 11.2 and 11.8 cm/s, the flux had a maximum midway down the bed and so the initial segregation process is most active there. In contrast, at lower air velocities u = 9.2 and 9.8 cm/s, the segregation process is most active at the top of the bed where the particle flux was largest. The larger magnitude of the initial flux at u = 9.2 and 9.8 cm/s compared to that at u = 10.4, 11.2 and 11.8 cm/s thus accounts for faster increase in the segregation efficiency, E during earlier times as seen in the main plot in Fig. 4. However, the final segregation efficiency that can be achieved is higher: 95% vs 90% at higher air velocities. Such behavior therefore opens the possibility to optimize segregation in terms of time and energy expended by varying the air velocity as segregation progresses.

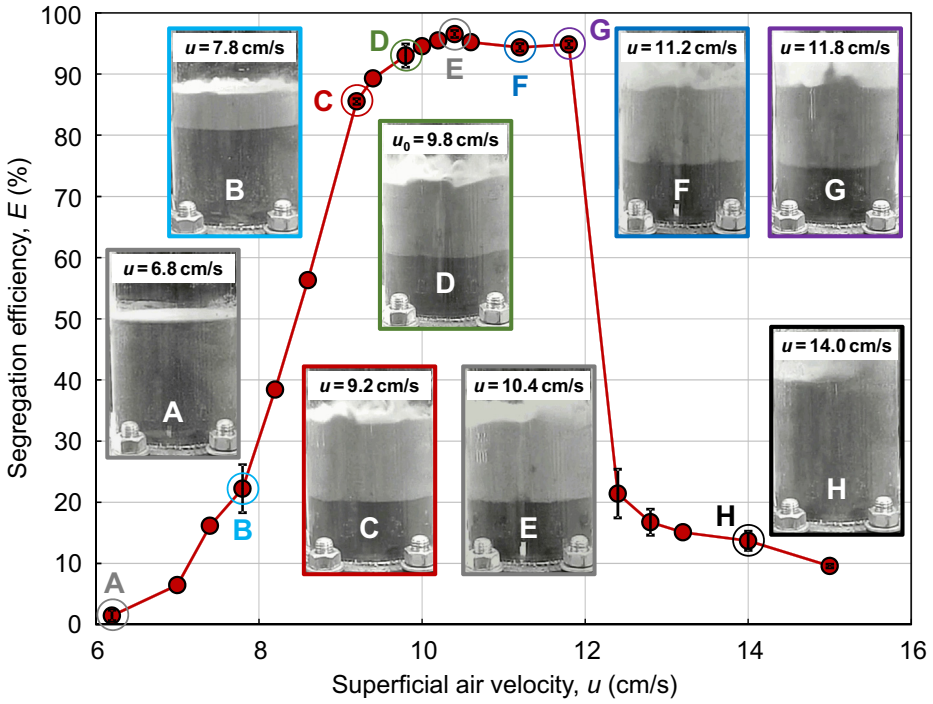

Fig. 3. Variation of the segregation efficiency, E with superficial velocity, u. Photos of the initially well-mixed 50:50 glass beads (white) and iron powder (black) bed after an aeration time of 600 s corresponding to the data points marked as A–H.

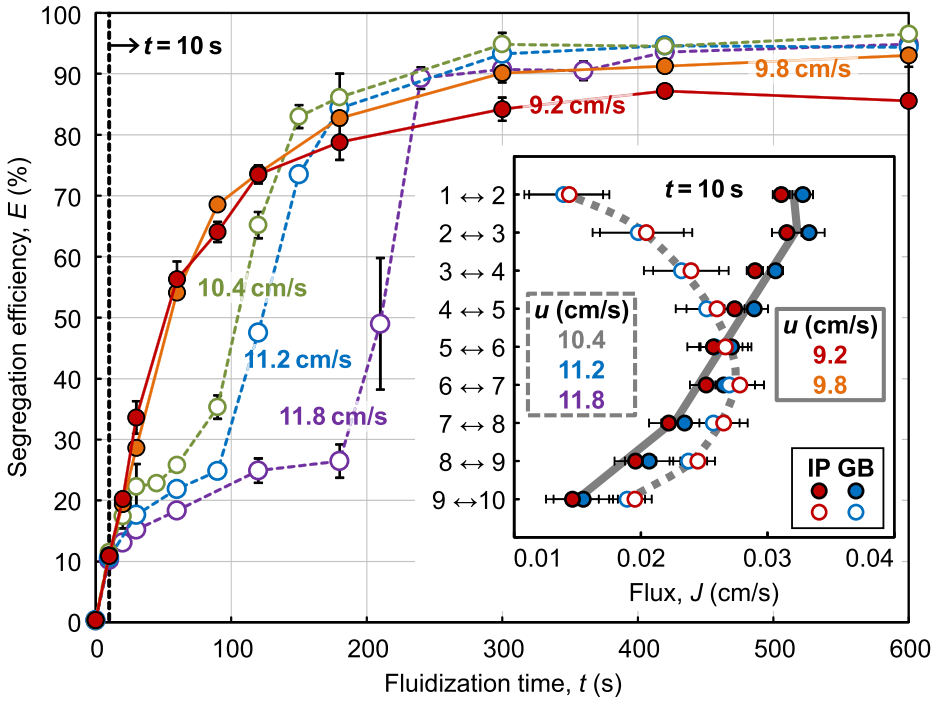

Fig. 4. Variation of the segregation efficiency, E with fluidization time at different superficial velocities, u for an initially well-mixed 50:50 glass beads (GB) and iron powder (IP) at the indicated superficial velocities, u: solid symbols −9.2 and 9.8 cm/s, open symbols −10.4, 11.2 and 11.8 cm/s. Inset: Variation of the average flux, J of GB and IP during the initial 10 s of aeration between layer L and $(L + 1)$ where $L = 1$ is the layer at the top 10% of the bed and $L = 10$ is the layer at the bottom 10% of the bed. The solid and broken lines are drawn to guide the eye.

Whereas most studies of the segregation of powder mixtures focused on the distinctive 2D or 3D spatial patterns of the segregated state, practical requirements of segregation are that the final phases are of high purity and are well separated spatially to facilitate easy extraction. This report is concerned with how this may be achieved for a 50:50 mixture of non-cohesive powders of identical size by using aeration. Starting from a well-mixed chaotic state, near total order of complete segregation can be achieved within a defined range of air velocity. And within this velocity range, differences in the rate of separation and the final efficiency that is attained can be exploited to optimize the operational efficiency of the separation process.

Although it is true that segregation reduces the entropy of the powder system, the total entropy of the process must have increased. The dynamic performance is quantified in terms of the time required and the degree of segregation that can be achieved. The time dependence of the segregation efficiency, E shown in Fig. 4 for such a simple, well-characterized system is likely to be useful in modelling studies such as computer simulations based on the discrete element method.

At low aeration velocities from just above the minimum fluidization velocity of the 50:50 mixture, at u_{mf} = 6 cm/s up to 9 cm/s – cases A to C in Fig. 3, partial segregation is still possible with the segregation efficiency, E being an increasing function of the air velocity in this range. Such observations suggest that within this lower air velocity range, complete segregation cannot be achieved because at some local position, the initially random bed evolved into the fixed bed regime (see Fig. 1) and thereby halting the segregation process. The details of how this may occur will be the subject of a future study. At present, it is sufficient to note that the segregation process is clearly complex and rich in details and more can be learned, for example, by studying the effects of using an initial composition that is not a 50:50 mixture, by using a liquid rather than air as the fluidizing medium or by considering systems in which inter-particle cohesion cannot be neglected. Also, there is much interesting physics in the behavior of powder beds gently aerated below the minimum fluidization velocity [15].

Acknowledgements

This work was supported in part by JSPS KAKENHI Grant Number JP18H03406 to Jun Oshitani, and the Australian Research Council through a Discovery Project Grant to Derek Y.C. Chan.

Appendix A. Supplementary material

Supplementary data to this article can be found online at https://doi.org/10.1016/j.apt.2019.12.002.

References

[1] National Research Council, Condensed matter and material physics: the science of the world around us, National Academies Press, 2007.
[2] M.E. Möbius, B.E. Lauderdale, S.R. Nagel, H.M. Jaeger, Brazil-nut effect: Size separation of granular particles, Nature 414 (2001), 270-270.
[3] X. Yan, Q. Shi, M. Hou, K. Lu, C.K. Chan, Effects of air on the segregation of particles in a shaken granular bed, Phys. Rev. Lett. 91 (2003) 014302.
[4] H.A. Makse, S. Havlin, P.R. King, H.E. Stanley, Spontaneous stratification in granular mixtures, Nature 386 (1997) 379–382.
[5] N. Jain, J.M. Ottino, R.M. Lueptow, Effect of interstitial fluid on a granular flowing layer, J. Fluid Mech. 508 (2004) 23–44.
[6] S. Ahmed, S.E. John, I.D. Sutalo, G. Metcalfe, K. Liff-man, Experimental study of density segregation at end walls in a horizontal rotating cylinder saturated with fluid: friction to lubrication transition, Granular Matter 14 (2012) 319–332.
[7] R. Vehring, Pharmaceutical particle engineering via spray drying, Pharm. Res. 25 (2008) 999–1022.
[8] S. Mitchell, N.L. Michels, J. Perez-Ramirez, From powder to technical body: the undervalued science of catalyst scale up, Chem. Soc. Rev. 42 (2013) 6094–6112.
[9] J. Oshitani, M. Ohnishi, M. Yoshida, G.V. Franks, Y. Kubo, S. Nakatsukasa, Dry separation of particulate iron ore using density-segregation in a gas-solid fluidized bed, Adv. Powder Technol. 24 (2013) 554–559.
[10] J. Oshitani, K. Teramoto, M. Yoshida, Y. Kubo, S. Nakatsukasa, G.V. Franks, Dry beneficiation of fine coal using density-segregation in a gas-solid fluidized bed, Adv. Powder Technol. 27 (2016) 1689–1693.
[11] J.R. Cui, E. Forssberg, Mechanical recycling of waste electric and electronic equipment: a review, J. Hazard. Mater. 99 (2003) 243–263.
[12] J. Li, H. Lu, J. Guo, Z.M. Xu, Y.H. Zhou, Recycle technology for recovering resources and products from waste printed circuit boards, Environ. Sci. Technol. 41 (2007) 1995–2000.
[13] P. Jop, Y. Forterre, O. Pouliquen, A constitutive law for dense granular flows, Nature 441 (2006) 727–730.
[14] P.C. Carman, Fluid flow through granular beds, Trans. Inst. Chem. Eng. Lond. 15 (1937) 150–166.
[15] J. Oshitani, T. Sasaki, T. Tsuji, K. Higashida, D.Y.C. Chan, Anomalous sinking of spheres due to local fluidization of apparently fixed powder beds, Phys. Rev. Lett. 116 (2016) 068001.